

Searching for a $P_{cs}(4200)$ state in the $\Lambda_b \rightarrow \phi\eta_c\Lambda$ reaction

Wen-Tao Lyu^{1, 2,*} and Eulogio Oset^{2, †}

¹*School of Physics, Zhengzhou University, Zhengzhou 450001, China*

²*Departamento de Física Teórica and IFIC, Centro Mixto Universidad de Valencia-CSIC Institutos de Investigación de Paterna, 46071 Valencia, Spain*

(Dated: January 29, 2026)

We propose the $\Lambda_b \rightarrow \phi\eta_c\Lambda$ reaction to observe a P_{cs} state around 4200 MeV, predicted at lower masses than expected from comparison with the P_c states, stemming as a consequence of the important role played by coupled channels in the P_{cs} case, which does not appear in the P_c case. That state decays to $\eta_c\Lambda$ with a width of about 200 keV. The reaction is related to $\Lambda_b^0 \rightarrow \phi D_s^-\Lambda_c^+$, which has already been observed. We predict a branching fraction for $\Lambda_b \rightarrow \phi P_{cs}(4200); P_{cs} \rightarrow \eta_c\Lambda$ of the order of 10^{-5} , which is within present capabilities of the LHCb collaboration. The observation of this state would bring valuable light on the nature of the P_c and P_{cs} states and the role played by coupled channels in hadron structure and hadron reactions.

I. INTRODUCTION

The discovery of the pentaquark P_c and P_{cs} states gave a boost to hadron physics, showing evidence of baryon states with more than three quarks, rather than three in conventional baryons [1–5]. The discovery of these states gave a boost to the molecular picture of many baryon states, given the accurate prediction of the existence of these states based on the interaction of mesons and baryons [6–10]. There has been extensive work on the issue after the discovery of these states, which are reviewed in different papers [11–16].

In the present work we concentrate on the P_{cs} states where there is still some debate concerning the nature of the observed states. While there is a broad consensus about the P_c states, this is not the case of the P_{cs} states, as we shall see. The $P_c(4312)$ state is associated to a $\bar{D}\Sigma_c$ molecule, while $P_c(4440)$, $P_c(4457)$ are associated to the $\bar{D}^*\Sigma_c$ molecule with $J^P = 1/2^-, 3/2^-$, with small mixture with other coupled channels, and some debate about the spin $1/2^-$ or $3/2^-$ association to the $P_c(4440)$ and $P_c(4457)$ [17–36].

The P_{cs} states have attracted less attention. The $P_{cs}(438)$ and $P_{cs}(4459)$ are associated to $\bar{D}\Xi_c$ and $\bar{D}^*\Xi_c$ molecular state by analogy to the $\bar{D}\Sigma_c$ and $\bar{D}^*\Sigma_c$ structures of the P_c states [37–46]. In Ref. [47], starting from a quark model structure, the molecular substructure was also studied, associating the $P_{cs}(4459)$ to $\bar{D}\Sigma_c$ mostly, and the $P_{cs}(4438)$ to a mixture of many molecular configurations. However, there is a drastic difference of the P_c and P_{cs} states concerning the molecular structure, because while the P_c states are mostly single channel states, with very small admixture with other coupled channels, this is not the case for the P_{cs} states, which was earlier noted in [42]. This issue has been further elaborated in [48]. Indeed, by looking at the coupled channels interaction for the P_c states studied in [23], one observes that

the $\bar{D}\Sigma_c$ and $\bar{D}\Lambda_c$ channels do not couple (see Eq. (3) of [23]), and similarly $\bar{D}^*\Sigma_c$ and $\bar{D}^*\Lambda_c$ do not mix (see Eqs. (4) and (6) of [23]). On the other hand, the $\bar{D}\Xi_c$ and $\bar{D}_s\Lambda_c$ states couple strongly in the formation of P_{cs} states (see Table 1 of [48]), and so do the $\bar{D}^*\Xi_c$ and $\bar{D}_s^*\Lambda_c$ states (see Table 2 of [48]). The coupled channels are very important in molecular formation, since the presence of a coupled channel implies an additional interaction in the other channel proportional to the square of the transition potential [49, 50]. The transition potential in the case of the $\bar{D}_s\Lambda_c$ and $\bar{D}\Xi_c$, or $\bar{D}_s^*\Lambda_c$ and $\bar{D}^*\Xi_c$ channels is very strong and distorts the picture of the P_{cs} states compared with that of the P_c states. As a consequence of that, a picture emerged from the coupled channel approach of [48], in which the $P_{cs}(4338)$ state was associated to the $\bar{D}^*\Sigma_c$ (with some mixture of $\bar{D}_s^*\Lambda_c$), and the $P_{cs}(4459)$ to $\bar{D}\Xi_c'$. Two more states emerged from that picture, a state around 4565 MeV coupling practically only to $\bar{D}^*\Xi_c'$ and another one coupling strongly to $\bar{D}\Xi_c$ (and also to $\bar{D}_s\Lambda_c$) which appears around 4200 MeV. The strong effect of the coupled channels lowers the energy of the state coupling to $\bar{D}\Xi_c$ with respect to its analog P_c state that couples to $\bar{D}\Sigma_c$. The coupled channels helping to build the $P_{cs}(4200)$ state are $\eta_c\Lambda$, $\bar{D}_s\Lambda_c$, $\bar{D}\Xi_c$ and $\bar{D}\Xi_c'$, and the couplings of the resonance to these channels are shown in Table I, together with the wave functions at the origin $g_i G_i$ [51]. As we can see, the main building blocks are $\bar{D}\Xi_c$ and $\bar{D}_s\Lambda_c$. The $\eta_c\Lambda$ couples weakly to the resonance, but having a mass lower than the resonance mass (4099 MeV), it is the natural decay channel of that state, but the $\bar{D}_s\Lambda_c$ is the channel which we will consider in order to produce the resonance. Since the coupling to $\eta_c\Lambda$ is so small, the width of the resonance is small, around 200 keV.

One might think that the small coupling to $\eta_c\Lambda$, the channel where the resonance will be observed, should make the signal of this resonance very small in any reaction, but we shall see that this is not the case, because in the reaction that we propose we produce the resonance with the $\bar{D}_s\Lambda_c$ channel off shell, and hence, the production of the resonance is not linked to the $\eta_c\Lambda$ channel. Once produced it will decay, in this case in $\eta_c\Lambda$, but the

* lvwentao9712@163.com

† oset@ific.uv.es

TABLE I. Couplings and wave functions of the again [in MeV] for the different channels

Poles	$\eta_c \Lambda$	$\bar{D}_s \Lambda_c$	$\bar{D} \Xi_c$	$\bar{D} \Xi'_c$
$4198.94 + i0.11$	$g_i \quad 0.12 - i0.00$	$3.01 - i0.01$	$4.85 + i0.01$	$0.01 - i0.03$
	$g_i G_i^{II} \quad -0.35 + i1.01$	$-19.24 + i0.05$	$-20.35 - i0.07$	$-0.03 + i0.09$

probability to find the resonance in $\eta_c \Lambda$ is the production probably of the P_{cs} , because this is the only decay channel. It is then not surprising that we obtain a branching ratio for the $P_c(4200)$ state which is relatively large.

The reaction that we propose is $\Lambda_b \rightarrow \phi \eta_c \Lambda$. The reason to propose that reaction is that the $\Lambda_b^0 \rightarrow \phi D_s^- \Lambda_c^+$ reaction has already been observed in [52]. The reaction is $\Lambda_b^0 \rightarrow \Lambda_c^+ D_s^- K^+ K^-$, but the $K^+ K^-$ come mostly from ϕ decay. Experimentally one finds [52]

$$\frac{\mathcal{B}r(\Lambda_b \rightarrow \Lambda_c \bar{D}_s \phi)}{\mathcal{B}r(\Lambda_b \rightarrow \Lambda_c \bar{D}_s)} \sim 10^{-2}, \quad (1)$$

which together with the branching fraction of the $\Lambda_b \rightarrow \Lambda_c \bar{D}_s$, which is of the order of 10^{-2} [53], gives

$$\mathcal{B}r(\Lambda_b \rightarrow \Lambda_c \bar{D}_s \phi) \sim 10^{-4}. \quad (2)$$

II. FORMALISM

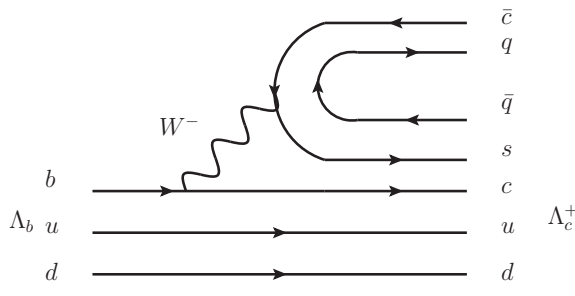


FIG. 1. $\Lambda_b \rightarrow \Lambda_c \bar{c} s$, together with hadronization of the $s\bar{c}$ component.

It is interesting to see how the $\Lambda_b^0 \rightarrow \Lambda_c^+ D_s^- \phi$ reaction can proceed at the microscopical level. We can see that in Fig. 1 with external emission. The $s\bar{c}$ pair in Fig. 1 hadronizes as

$$s\bar{c} \Rightarrow \sum_i s\bar{q}_i q_i \bar{c} = \sum_i M_{3i} M'_{i4} = (MM')_{34},$$

where M_{ij} , M'_{ij} are $q_i \bar{q}_j$ matrices written in terms of mesons, pseudoscalar or vectors. We have

$$P = \begin{pmatrix} \frac{\pi^0}{\sqrt{2}} + \frac{\eta}{\sqrt{3}} + \frac{\eta'}{\sqrt{6}} & \pi^+ & K^+ & \bar{D}^0 \\ \pi^- & -\frac{\pi^0}{\sqrt{2}} + \frac{\eta}{\sqrt{3}} + \frac{\eta'}{\sqrt{6}} & K^0 & D^- \\ K^- & \bar{K}^0 & -\frac{\eta}{\sqrt{3}} + \frac{2\eta'}{\sqrt{6}} & D_s^- \\ D^0 & D^+ & D_s^+ & \eta_c \end{pmatrix} \quad (3)$$

$$V = \begin{pmatrix} \frac{\rho^0}{\sqrt{2}} + \frac{\omega}{\sqrt{2}} & \rho^+ & K^{*+} & \bar{D}^{*0} \\ \rho^{*-} & -\frac{\rho^0}{\sqrt{2}} + \frac{\omega}{\sqrt{2}} & K^{*0} & D^{*-} \\ K^{*-} & \bar{K}^{*0} & \phi & D_s^{*-} \\ D^{*0} & D^{*+} & D_s^{*+} & J/\psi \end{pmatrix}, \quad (4)$$

We need to hadronize $s\bar{c}$ into a pseudoscalar meson and a vector and we can have

$$(PV)_{34} : s\bar{c} \rightarrow (PV)_{34}, \quad (5)$$

$$(VP)_{34} : s\bar{c} \rightarrow (VP)_{34}, \quad (6)$$

$$(PV)_{34} = (K^- \bar{D}^{*0} + \bar{K}^0 \bar{D}^{*-} - \frac{1}{\sqrt{3}} \eta D_s^{*-} + \dots), \quad (7)$$

$$(VP)_{34} = (K^{*-} \bar{D}^0 + \bar{K}^{*0} D^- + \phi D_s^- + \dots), \quad (8)$$

where the dots indicate states with extra $c\bar{c}$ quarks not relevant in our study. We can see that the $(VP)_{34}$ contribution gives rise to $\Lambda_c^0 \rightarrow \Lambda_c^+ \phi D_s^-$.

Once $\Lambda_c^+ D_s^-$ is produced, we can obtain $\Lambda_b^0 \rightarrow \phi \eta_c \Lambda$ through rescattering of the $\Lambda_c^+ D_s^-$ component as shown in Fig. 2.

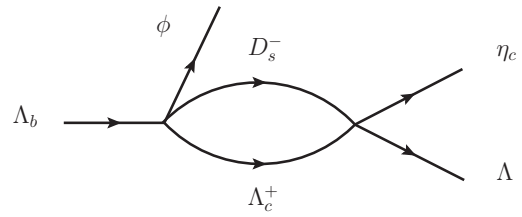


FIG. 2. Rescattering of $D_s^- \Lambda_c^+$ to $\eta_c \Lambda$, mediated by the resonance $P_{cs}(4200)$.

There is another mechanism to produce $\eta_c \Lambda \phi$ through internal emission, as shown in Fig. 3. The mechanism of Fig. 3 is color suppressed and would have a reduction peak of about $1/N_c$ with respect to $\Lambda_b^0 \rightarrow \phi D_s^- \Lambda_c^+$. We, thus, have the tree level production of Fig. 3(b) together with the rescattering mechanism of Fig. 2, corresponding to a production amplitude for $\Lambda_b \rightarrow \phi \eta_c \Lambda$

$$t = A\beta + AG_{\bar{D}_s \Lambda_c}(M_{\text{inv}}(\eta_c \Lambda))t_{\bar{D}_s \Lambda_c, \eta_c \Lambda}(M_{\text{inv}}(\eta_c \Lambda)), \quad (9)$$

with $\beta \sim 1/N_c$ and A the vertex $\Lambda_b^0 \rightarrow \phi D_s^- \Lambda_c^+$. In Eq. (9) G is the loop function of the $D_s^- \Lambda_c^+$ propagation of Fig. 2, which is calculated in [48] and is regularized with cut off regularization. We use the information of [48], but the needed information is already available

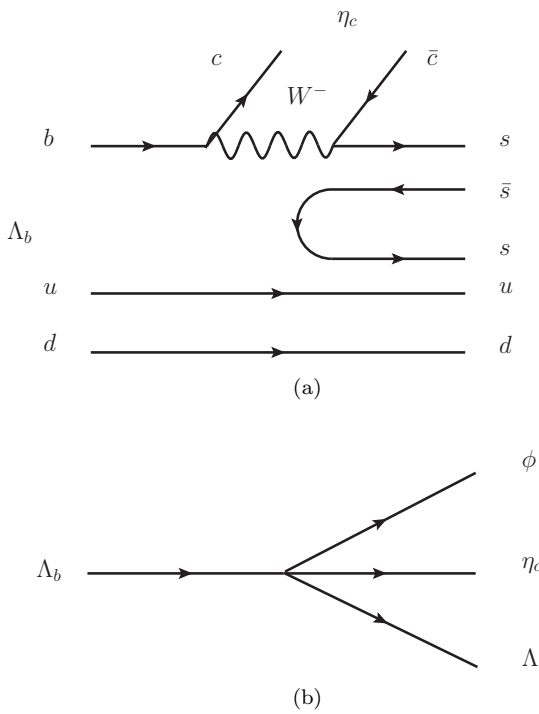


FIG. 3. (a) Mechanism to produce $\eta_c \phi \Lambda$ in Λ_b decay through internal emission. (b) The mechanism depicted as a tree level diagram.

in Table I. Indeed, we can write the $t_{\bar{D}_s \Lambda_c, \eta_c \Lambda}$ amplitude corresponding to the $P_{cs}(4200)$ resonance as

$$t_{\bar{D}_s \Lambda_c, \eta_c \Lambda} = \frac{g_{\bar{D}_s \Lambda_c} g_{\eta_c \Lambda}}{M_{\text{inv}}(\eta_c \Lambda) - M_{P_{cs}} + i \frac{\Gamma_{P_{cs}}}{2}}. \quad (10)$$

Then in the contribution $G_{\bar{D}_s \Lambda_c} t_{\bar{D}_s \Lambda_c, \eta_c \Lambda}$ we will have $G_{\bar{D}_s \Lambda_c} g_{\bar{D}_s \Lambda_c}$, which is the $\bar{D}_s \Lambda_c$ wave function of the origin of the $\bar{D}_s \Lambda_c$ channel and is tabulated in Table I, together with $g_{\eta_c \Lambda}$ and $\Gamma_{P_{cs}}/2$ (imaginary part of the pole position, 0.11 MeV). We need the value of A in Eq. (9) to obtain the branching ratio in absolute terms. We evaluate it as follows.

A. Extraction of A from the $\Lambda_b^0 \rightarrow \phi D_s^- \Lambda_c^+$ reaction

We must contract the polarization of the ϕ , $\vec{\epsilon}_\phi$, with some vector. We choose one combination $\vec{\epsilon}_\phi \cdot \vec{\sigma}$ with $\vec{\sigma}$ the spin operator acting on the baryons. Other choices can be done, but since this is propagated in the diagrams of Fig. 2, it simply leads to a factor which is common to all processes and disappears in the ratios that we construct.

The decay width for the process $\Lambda_b^0 \rightarrow \phi D_s^- \Lambda_c^+$ is given by

$$\frac{d\Gamma}{dM_{\text{inv}}(\bar{D}_s \Lambda_c)} = \frac{1}{(2\pi)^3} \frac{2M_{\Lambda_c} 2M_{\Lambda_b}}{4M_{\Lambda_b}^2} p_\phi \tilde{p}_{\bar{D}_s} \sum \sum |t'|^2, \quad (11)$$

with $t' = A \vec{\sigma} \vec{\epsilon}_\phi$, and

$$p_\phi = \frac{\lambda^{1/2}(M_{\Lambda_b}^2, m_\phi^2, M_{\text{inv}}^2(\bar{D}_s \Lambda_c))}{2M_{\Lambda_b}}, \quad (12)$$

$$\tilde{p}_{\bar{D}_s} = \frac{\lambda^{1/2}(M_{\text{inv}}^2(\bar{D}_s \Lambda_c), m_{\bar{D}_s}^2, M_{\Lambda_c}^2)}{2M_{\text{inv}}(\bar{D}_s \Lambda_c)}. \quad (13)$$

The sum and average over the spins of the Λ_b , Λ_c gives

$$\begin{aligned} \overline{\sum \sum |t'|^2} &= \frac{1}{2} \sum_{\epsilon_{\text{pol}}} \sum_m \sum_{m'} \langle m | \sigma_i \epsilon_i | m' \rangle \langle m' | \sigma_j \epsilon_j | m \rangle A^2 \\ &= \frac{1}{2} \sum_{\epsilon_{\text{pol}}} \sum_m \langle m | \delta_{ij} + i \epsilon_{ijk} \sigma_k | m \rangle A^2 \epsilon_i \epsilon_j \\ &= A^2 \delta_{ij} \delta_{ij} \\ &= 3A^2. \end{aligned} \quad (14)$$

Integrating Eq. (11) over $M_{\text{inv}}(\bar{D}_s \Lambda_c)$ and comparing the result with the branching fraction of Eq. (2) we obtain the value of A^2/Γ_{Λ_b} which is

$$\frac{A^2}{\Gamma_{\Lambda_b}} = 2.23 \times 10^{-10} \text{ MeV}^{-3}. \quad (15)$$

B. Branching ratio for $\Lambda_b \rightarrow \phi \eta_c \Lambda$

Next, we can evaluate the branching ratio from $\Lambda_b \rightarrow \phi \eta_c \Lambda$. We have

$$\frac{d\Gamma}{dM_{\text{inv}}(\eta_c \Lambda)} = \frac{1}{(2\pi)^3} \frac{M_\Lambda}{M_{\Lambda_b}} p_\phi \tilde{p}_{\eta_c} |t|^2 \cdot 3, \quad (16)$$

with t given by Eq. (9), with

$$p_\phi = \frac{\lambda^{1/2}(M_{\Lambda_b}^2, m_\phi^2, M_{\text{inv}}^2(\eta_c \Lambda))}{2M_{\Lambda_b}}, \quad (17)$$

$$\tilde{p}_{\eta_c} = \frac{\lambda^{1/2}(M_{\text{inv}}^2(\eta_c \Lambda), m_{\eta_c}^2, M_\Lambda^2)}{2M_{\text{inv}}(\eta_c \Lambda)}, \quad (18)$$

and to calculate the branching ratio we divide by Γ_{Λ_b} , and for that we use A^2/Γ_{Λ_b} of Eq. (15).

III. RESULTS

In Fig. 4¹, we observe a very narrow peak corresponding to the narrow $P_{cs}(4200)$ resonance. If we integrate

¹ Around 4350 MeV, far away from the resonance peak, we take the prescription of [54] to write $G_{\bar{D}_s \Lambda_c} = \text{Re}(G_{\bar{D}_s \Lambda_c}) + i\text{Im}(G_{\bar{D}_s \Lambda_c})$ with $q_{\text{max}} = 600$ MeV from [48], taking $\text{Re}(G_{\bar{D}_s \Lambda_c}) = 0$ if it becomes positive and the exact expression for $\text{Im}(G_{\bar{D}_s \Lambda_c})$. Alternatively, we can use gG for $\bar{D}_s \Lambda_c$ at the pole, tabulated in Table I, and the results are basically the same.

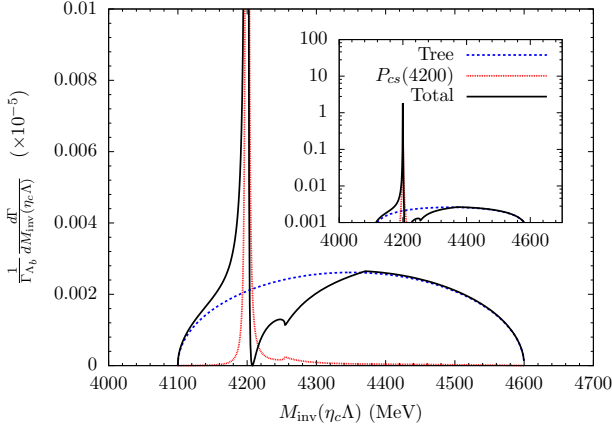


FIG. 4. $\frac{1}{\Gamma_{\Lambda_b}} \frac{d\Gamma}{dM_{\text{inv}}(\eta_c\Lambda)}$ as a function of $M_{\text{inv}}(\eta_c\Lambda)$ for the $\Lambda_b \rightarrow \phi\eta_c\Lambda$.

over the whole $\eta_c\Lambda$ invariant mass range we obtain

$$\frac{\Gamma_{\Lambda_b \rightarrow \phi\eta_c\Lambda}}{\Gamma_{\Lambda_b}} \simeq 3.8 \times 10^{-5}, \quad (19)$$

well within measurable rates for Λ_b decays reported in the PDG [53]. It is instructive to see the rate obtained for the resonance peak. Integrating in the range $M_{P_{cs}} - 2\Gamma_{P_{cs}}$, $M_{P_{cs}} + 2\Gamma_{P_{cs}}$, we obtain

$$\mathcal{Br}[\Lambda_b \rightarrow \phi P_{cs}(4200)] \simeq 2.46 \times 10^{-5}. \quad (20)$$

It is interesting to see that this rate does not depend on $g_{\eta_c\Lambda}$, the small coupling of the resonance to the $\eta_c\Lambda$ decay channel. Indeed, the resonance part of the width will come from the Gt term of Eq. (9). Then

$$\begin{aligned} |t_{\bar{D}_s\Lambda_c, \eta_c\Lambda}|^2 &= \frac{g_{\bar{D}_s\Lambda_c}^2 g_{\eta_c\Lambda}^2 A^2 G_{\bar{D}_s\Lambda_c}^2}{(M_{\text{inv}}(\eta_c\Lambda) - M_{P_{cs}})^2 + \left(\frac{\Gamma_{P_{cs}}}{2}\right)^2} \\ &= A^2 (g_{\bar{D}_s\Lambda_c} G_{\bar{D}_s\Lambda_c})^2 g_{\eta_c\Lambda}^2 \left(-\frac{2}{\Gamma_{P_{cs}}}\right) \\ &\quad \times \text{Im} \left(\frac{1}{M_{\text{inv}}(\eta_c\Lambda) - M_{P_{cs}} + i\frac{\Gamma_{P_{cs}}}{2}} \right) \\ &\simeq A^2 (g_{\bar{D}_s\Lambda_c} G_{\bar{D}_s\Lambda_c})^2 g_{\eta_c\Lambda}^2 \left(-\frac{2}{\Gamma_{P_{cs}}}\right) (-\pi) \\ &\quad \times \delta(M_{\text{inv}}(\eta_c\Lambda) - M_{P_{cs}}), \end{aligned} \quad (21)$$

where we have used that $\text{Im}(x - x_0 + i\epsilon) = -\pi\delta(x - x_0)$, which upon integration over M_{inv} , and summing over spins and ϕ polarizations, gives

$$\begin{aligned} \mathcal{Br}[\Lambda_b \rightarrow \phi P_{cs}(4200)] &= \frac{1}{(2\pi)^3} \frac{M_\Lambda}{M_{\Lambda_b}} p_\phi \tilde{p}_{\eta_c} 3A^2 \\ &\quad \times (g_{\bar{D}_s\Lambda_c} G_{\bar{D}_s\Lambda_c})^2 g_{\eta_c\Lambda}^2 \frac{2\pi}{\Gamma_{P_{cs}}}, \end{aligned} \quad (22)$$

with $p_\phi, \tilde{p}_{\eta_c}$ calculated at $M_{\text{inv}}(\eta_c\Lambda) = M_{P_{cs}}$. Since $\Gamma_{P_{cs}}$ is proportional to $g_{\eta_c\Lambda}^2$, the coupling $g_{\eta_c\Lambda}$ disappears in

the formula of Eq. (22). One can go one step forward and considering that

$$\Gamma_{P_{cs}} = \frac{1}{8\pi} \frac{2M_\Lambda 2M_{P_{cs}}}{M_{P_{cs}}^2} g_{\eta_c\Lambda}^2 \tilde{p}_{\eta_c}, \quad (23)$$

we obtain

$$\Gamma_{\Lambda_b \rightarrow \phi P_{cs}} = \frac{1}{8\pi} \frac{2M_\Lambda 2M_{P_{cs}}}{M_{\Lambda_b}^2} 3A^2 (g_{\bar{D}_s\Lambda_c} G_{\bar{D}_s\Lambda_c})^2 p_\phi, \quad (24)$$

which corresponds to the production of the P_{cs} resonance with coalescence production depicted in Fig. 5. Hence,

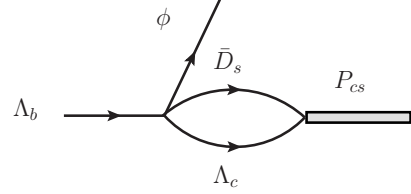


FIG. 5. Coalescence P_{cs} production in $\Lambda_b \rightarrow \phi P_{cs}$ driven by the $\bar{D}_s\Lambda_c$ intermediate state.

it is proved that the small coupling of the resonance $P_{cs}(4200)$ to $\eta_c\Lambda$ is no obstacle to having a large branching ratio. Only the small width of $\Gamma_{P_{cs}} = 0.22$ MeV will pose experimental difficulties, but small widths of this type are measured in experiments of LHCb like in the observation of the T_{cc} states [55, 56].

The result obtained with Eq. (24) gives $\mathcal{Br}[\Lambda_b \rightarrow \phi P_{cs}] = 2.47 \times 10^{-5}$, basically the same calculated in Eq. (20). If the resolution of an experiment is bigger than this width, the spectrum will be seen wider but the integrated width will be the same. Branching ratios of 10^{-5} are common in Λ_b decay [53], where even branching ratios of 10^{-7} are reported. Hence, the proposed experiment is well within the LHCb capabilities at present, and certainly in future runs of the LHCb.

IV. CONCLUSIONS

We propose here a reaction to detect a P_{cs} state predicted around 4200 MeV, not yet observed. This P_{cs} state at lower energy than expected from a comparison of the P_c states with the P_{cs} ones, stems because of the role played by coupled channels in the P_{cs} case which do not appear in the P_c case. The reaction proposed is $\Lambda_b \rightarrow \phi\eta_c\Lambda$. The motivation to propose this reaction is because the $\Lambda_b^0 \rightarrow \phi D_s^- \Lambda_c^+$ reaction has already been observed and the predicted $P_{cs}(4200)$ state couples strongly to $D_s^- \Lambda_c$ and $\bar{D} \Xi_c$. The coupling of the $P_{cs}(4200)$ state to $\eta_c\Lambda$ is very small, and this being the only decay channel, makes the width of that state very small. However, this is no obstacle to having large production rates, because the production of the resonance is driven by primarily

the $\Lambda_b^0 \rightarrow \phi D_s^- \Lambda_c^+$ reaction, where the resonance is produced which later decays in the $\eta_c \Lambda$ channel. We obtain branching ratios for the production of this resonance of the order of 10^{-5} , well within present LHCb capabilities, and we anticipate that it could be easily studied in new runs of the LHCb. The observation of this P_{cs} state with a mass lower than expected from comparison to the P_c states, would shed valuable light on the nature of the P_c and P_{cs} resonances and the important role played by coupled channels in the structure of hadrons and hadronic reactions.

ACKNOWLEDGMENTS

This work was supported by the National Key R&D Program of China (Grant No. 2024YFE0105200),

the Natural Science Foundation of Henan (Grant No. 252300423951), the National Natural Science Foundation of China (Grant No. 12475086), and the Zhengzhou University Young Student Basic Research Projects for PhD students (Grant No. ZDBJ202522). Wen-Tao Lyu acknowledges the support of the China Scholarship Council. This work is also partly supported by the Spanish Ministerio de Economía y Competitividad (MINECO) and European FEDER funds under Contracts No. FIS2017-84038-C2-1-PB, PID2020-112777GB-I00, and by Generalitat Valenciana under contract PROMETEO/2020/023. This project has received funding from the European Union Horizon 2020 research and innovation program under the program H2020-INFRAIA-2018-1, grant agreement No. 824093 of the STRONG-2020 project.

[1] R. Aaij *et al.* [LHCb], Phys. Rev. Lett. **115** (2015), 072001.

[2] R. Aaij *et al.* [LHCb], Phys. Rev. Lett. **122** (2019) no.22, 222001.

[3] R. Aaij *et al.* [LHCb], Sci. Bull. **66** (2021), 1278-1287.

[4] R. Aaij *et al.* [LHCb], Phys. Rev. Lett. **131** (2023) no.3, 031901.

[5] R. Aaij *et al.* [LHCb], Phys. Rev. Lett. **128** (2022) no.6, 062001.

[6] J. J. Wu, R. Molina, E. Oset and B. S. Zou, Phys. Rev. Lett. **105** (2010), 232001.

[7] J. J. Wu, R. Molina, E. Oset and B. S. Zou, Phys. Rev. C **84** (2011), 015202.

[8] J. J. Wu, T. S. H. Lee and B. S. Zou, Phys. Rev. C **85** (2012), 044002.

[9] C. W. Xiao, J. Nieves and E. Oset, Phys. Rev. D **88** (2013), 056012.

[10] M. Karliner and J. L. Rosner, Phys. Rev. Lett. **115** (2015) no.12, 122001.

[11] H. X. Chen, W. Chen, X. Liu and S. L. Zhu, Phys. Rept. **639** (2016), 1-121.

[12] R. F. Lebed, R. E. Mitchell and E. S. Swanson, Prog. Part. Nucl. Phys. **93** (2017), 143-194.

[13] F. K. Guo, C. Hanhart, U. G. Meißner, Q. Wang, Q. Zhao and B. S. Zou, Rev. Mod. Phys. **90** (2018) no.1, 015004 [erratum: Rev. Mod. Phys. **94** (2022) no.2, 029901].

[14] Y. R. Liu, H. X. Chen, W. Chen, X. Liu and S. L. Zhu, Prog. Part. Nucl. Phys. **107** (2019), 237-320.

[15] A. Ali, J. S. Lange and S. Stone, Prog. Part. Nucl. Phys. **97** (2017), 123-198.

[16] H. X. Chen, W. Chen, X. Liu, Y. R. Liu and S. L. Zhu, Rept. Prog. Phys. **86** (2023) no.2, 026201.

[17] Z. Y. Yang, J. Song, W. H. Liang and E. Oset, Eur. Phys. J. C **85**, no.9, 954 (2025)

[18] M. Z. Liu, Y. W. Pan, F. Z. Peng, M. Sánchez Sánchez, L. S. Geng, A. Hosaka and M. Pavon Valderrama, Phys. Rev. Lett. **122**, no.24, 242001 (2019)

[19] Z. H. Guo and J. A. Oller, Phys. Lett. B **793**, 144-149 (2019)

[20] M. L. Du, V. Baru, F. K. Guo, C. Hanhart, U. G. Meißner, J. A. Oller and Q. Wang, JHEP **08**, 157 (2021)

[21] R. Chen, Z. F. Sun, X. Liu and S. L. Zhu, Phys. Rev. D **100**, no.1, 011502 (2019)

[22] J. He, Eur. Phys. J. C **79**, no.5, 393 (2019)

[23] C. W. Xiao, J. Nieves and E. Oset, Phys. Rev. D **100**, no.1, 014021 (2019)

[24] L. Meng, B. Wang, G. J. Wang and S. L. Zhu, Phys. Rev. D **100**, no.1, 014031 (2019)

[25] M. Z. Liu, T. W. Wu, M. Sánchez Sánchez, M. P. Valderrama, L. S. Geng and J. J. Xie, Phys. Rev. D **103**, no.5, 054004 (2021)

[26] Y. Yamaguchi, H. García-Tecocoatzi, A. Giachino, A. Hosaka, E. Santopinto, S. Takeuchi and M. Takizawa, Phys. Rev. D **101**, no.9, 091502 (2020)

[27] M. Pavon Valderrama, Phys. Rev. D **100**, no.9, 094028 (2019)

[28] M. L. Du, Z. H. Guo and J. A. Oller, Phys. Rev. D **104**, no.11, 114034 (2021)

[29] H. Xu, Q. Li, C. H. Chang and G. L. Wang, Phys. Rev. D **101**, no.5, 054037 (2020)

[30] F. Z. Peng, J. X. Lu, M. Sánchez Sánchez, M. J. Yan and M. Pavon Valderrama, Phys. Rev. D **103**, no.1, 014023 (2021)

[31] C. W. Xiao, J. X. Lu, J. J. Wu and L. S. Geng, Phys. Rev. D **102**, no.5, 056018 (2020)

[32] F. Z. Peng, M. J. Yan, M. Sánchez Sánchez and M. P. Valderrama, Eur. Phys. J. C **81**, no.7, 666 (2021)

[33] M. Z. Liu, Y. W. Pan and L. S. Geng, Phys. Rev. D **103**, no.3, 034003 (2021)

[34] N. Yalikun, Y. H. Lin, F. K. Guo, Y. Kamiya and B. S. Zou, Phys. Rev. D **104**, no.9, 094039 (2021)

[35] Z. Y. Lin, J. B. Cheng, B. L. Huang and S. L. Zhu, Phys. Rev. D **108**, no.11, 114014 (2023)

[36] K. Chen, R. Chen, L. Meng, B. Wang and S. L. Zhu, Eur. Phys. J. C **82**, no.7, 581 (2022)

[37] F. L. Wang and X. Liu, Phys. Lett. B **835**, 137583 (2022)

[38] M. J. Yan, F. Z. Peng, M. Sánchez Sánchez and M. Pavon Valderrama, Phys. Rev. D **107**, no.7, 7 (2023)

[39] C. W. Xiao, J. Nieves and E. Oset, Phys. Lett. B **799**, 135051 (2019)

- [40] L. Meng, B. Wang and S. L. Zhu, Phys. Rev. D **107**, no.1, 014005 (2023)
- [41] A. Giachino, A. Hosaka, E. Santopinto, S. Takeuchi, M. Takizawa and Y. Yamaguchi, Phys. Rev. D **108**, no.7, 074012 (2023)
- [42] K. Chen, Z. Y. Lin and S. L. Zhu, Phys. Rev. D **106**, no.11, 116017 (2022)
- [43] J. T. Zhu, S. Y. Kong and J. He, Phys. Rev. D **107**, no.3, 034029 (2023)
- [44] K. Azizi, Y. Sarac and H. Sundu, Phys. Rev. D **108**, no.7, 074010 (2023)
- [45] H. W. Ke, F. Lu, H. Pang, X. H. Liu and X. Q. Li, Eur. Phys. J. C **83**, no.11, 1074 (2023)
- [46] Y. B. Shen, Z. W. Liu, M. Z. Liu, R. X. Shi, C. W. Xiao, W. H. Liang and L. S. Geng, [arXiv:2512.24247 [hep-ph]].
- [47] P. G. Ortega, D. R. Entem and F. Fernandez, Phys. Lett. B **838**, 137747 (2023)
- [48] A. Feijoo, W. F. Wang, C. W. Xiao, J. J. Wu, E. Oset, J. Nieves and B. S. Zou, Phys. Lett. B **839**, 137760 (2023)
- [49] T. Hyodo, Int. J. Mod. Phys. A **28**, 1330045 (2013)
- [50] F. Aceti, L. R. Dai, L. S. Geng, E. Oset and Y. Zhang, Eur. Phys. J. A **50**, 57 (2014)
- [51] D. Gammermann, J. Nieves, E. Oset and E. Ruiz Arriola, Phys. Rev. D **81**, 014029 (2010)
- [52] R. Aaij *et al.* [LHCb], Phys. Rev. D **112**, no.5, 052013 (2025)
- [53] S. Navas *et al.* [Particle Data Group], Phys. Rev. D **110**, no.3, 030001 (2024)
- [54] L. Roca, J. Song and E. Oset, [arXiv:2509.19840 [hep-ph]].
- [55] R. Aaij *et al.* [LHCb], Nature Phys. **18**, no.7, 751-754 (2022)
- [56] R. Aaij *et al.* [LHCb], Nature Commun. **13**, no.1, 3351 (2022)